Physica E 165 (2025) 116114

Contents lists available at ScienceDirect

Physica E: Low-dimensional Systems and Nanostructures

journal homepage: www.elsevier.com/locate/physe

Rogue-wave statistics in Anderson chains

M.F.V. Oliveira [a], A.M.C. Souza [b], M.L. Lyra [a,*], F.A.B.F. de Moura [a], G.M.A. Almeida [a]

[a] Instituto de Física, Universidade Federal de Alagoas, 57072-900 Maceió, AL, Brazil
[b] Departamento de Física, Universidade Federal de Sergipe, 49100-000 São Cristóvão, SE, Brazil

ARTICLE INFO

Editor: Rudolf A. Romer

Keywords:
Anderson localization
Rogue waves
Speckle statistics

ABSTRACT

The 1D Anderson model featuring uncorrelated diagonal disorder is considered. The wavefunction statistics associated to transitions between distinct locations is analyzed. In the presence of mild disorder, the local squared wavefunctions, that is occupation probabilities, obey exponential statistics. When disorder is high, amplitudes measured near the input site are well described by Rician distributions, a form of sub-exponential statistics, due to the influence of strongly localized modes. This results in a reduced likelihood of rogue wave events. When the statistics is taken over various disorder realizations or locations, the lack of knowledge over the rate of the exponential processes acting locally yields long-tailed distributions. As a consequence, rogue waves become more frequent at locations closer to the input for increasing disorder strength. Our findings can be used to assess the occurrence of extreme events as well as the degree of localization over a broad class of disordered models.

1. Introduction

Extreme events such as rogue waves are ubiquitous in many physical systems. From the ocean [1] to the optical domain [2], these events are unpredictable outliers yielding amplitudes far above the average [3]. As such, they can yield to hazardous consequences to ships and the like. Understanding their generation mechanism in detail either of linear and/or nonlinear models is thus paramount [4–14].

Linear rogue waves in particular are usually studied on disordered media [13,15–22]. Indeed, some degree of noise, whatever its origin, must be present to generate superposition of random complex amplitudes (phasors). Simple wave models predict that the resulting amplitude (squared) of those waves must obey Rayleigh (exponential) statistics in the asymptotic limit of a large number of uncorrelated phasors [23]. In optics, such condition is associated to a fully developed speckle. A distinct feature of extreme waves is therefore deviations that go beyond the exponential regime – the so-called L-shaped or heavy tailed statistics – when outliers occur more often than predicted [3].

Disordered systems are ubiquitous in condensed-matter physics. The theory of Anderson localization [24] establishes that the wavefunction of a single particle will be exponentially localized for any amount of uncorrelated disorder in 1D and 2D lattices. The interplay between localization and the onset of rogue waves has been gaining interest recently [21,22,25] (see also [26]). We also remark that deviations from Rayleigh statistics in random media has been studied for decades in radiation scattering [27,28].

Our focus here is to explore anomalous fluctuations and their associated statistics in standard Anderson chains. We discuss how a given speckle behavior emerges due to the presence of localized states under the influence of diagonal (on-site) disorder. By mapping the quantum time evolution onto a random phasor sum model, we use speckle theory [23] to analyze the specific role of the disorder on the statistics of intensities $I = |\Psi|^2$. We will see that the distance from the input site plays an important role in the prediction of rogue waves. The closer the probe is to the source, those events should occur less frequently than predicted by exponential statistics for a time series acquired for a given disorder sample. In this case the intensities are found to assume Rician-type distributions. Long-tailed distributions arise when the data pertaining to distinct disorder realizations and/or different output locations are jointly considered. We show that as those distributions raise the rogue-wave intensity threshold with the disorder strength W, making such events rarer to occur at locations farther from the source.

2. Model and methods: Speckles from Hamiltonian time evolution

In this section we introduce the Anderson model and prepare the ground for the speckle analogue of its dynamics. For the general reader that has never had any contact with the speckle theory, we refer to the excellent book in [23]. Now, consider a single particle hopping in a N-site linear chain with periodic boundary conditions. The corresponding

* Corresponding author.
E-mail address: marcelo@fis.ufal.br (M.L. Lyra).

https://doi.org/10.1016/j.physe.2024.116114
Received 31 May 2024; Received in revised form 24 September 2024; Accepted 24 September 2024
Available online 28 September 2024

Hamiltonian is ($\hbar = 1$)

$$H = \sum_{n=1}^{N} \epsilon_n a_n^\dagger a_n - \sum_{\langle n,m \rangle} J_{n,m} a_m^\dagger a_n, \tag{1}$$

where $J_{n,m}$ is the nearest-neighbor hopping strength, ϵ_n is the disordered local potential, and a_n ($a_n^\dagger$) is the particle creation (annihilation) operator for the nth site. Let us set the hopping strength uniform along the lattice, $J_{n,m} = J$ (hereafter defined as our standard energy unit), and ϵ_n as a random variable uniformly distributed in $[-W/2, W/2]$, with W being the disorder width.

When we consider a delta-like initial state $|\psi(0)\rangle = |n_0\rangle$, its quantum time evolution reads

$$|\psi(t)\rangle = e^{-iHt}|n_0\rangle = \sum_k e^{-iE_k t} v_{k,n_0} |E_k\rangle, \tag{2}$$

where $|E_k\rangle$ and E_k are the eigenstates and eigenvalues of the Hamiltonian, respectively, with $v_{k,n} = \langle n|E_k\rangle$ (assumed to be real).

In the 1D Anderson model featuring diagonal uncorrelated disorder, all eigenstates are expected to be exponentially localized for any amount of disorder in the thermodynamic limit. It means that the eigenstates amplitudes are all of the form $v_{k,n} \propto e^{-|n-n_k|/\xi_k}$, each k being related to a different n_k. The factor ξ_k is the so-called localization length and accounts for how large the eigenstate tail is. In turn, the eigenvalues E_k are also randomly distributed with respect to the typical density of states displayed by Anderson arrays. In the long-time regime and considering time intervals $\Delta t J \gg 1$ the phases $\phi_k(t) = -E_k t$ (modulo 2π) can be effectively regarded as random variables uniformly distributed in $(0, 2\pi)$. The local wavefunction can finally be cast as the random phasor sum

$$\psi(n,t) = \langle n|\psi(t)\rangle = \sum_{k=1}^{N} a_k e^{i\phi_k(t)}, \tag{3}$$

with constant coefficients $a_k = a_k(n_0, n) = v_{k,n_0} v_{k,n}$ (for a given disorder distribution) and phases $\phi_k(t)$ that are effectively random over time.

The equation above is the standard description for optical speckles. Assuming that all a_k are equal and the phases ϕ_k are i.i.d. random variables, we know that as $N \to \infty$, the central limit theorem leads to a joint circular Gaussian distribution for $\mathrm{Re}\{\psi\}$ and $\mathrm{Im}\{\psi\}$ centered at the origin of the complex plane. As a consequence, the resultant amplitude $|\psi|$ is Rayleigh distributed and the intensity $I = |\psi|^2$ obeys the exponential distribution

$$p(I) = s^{-1} e^{-I/s}, \tag{4}$$

with $s = \langle I \rangle$. This outcome holds for any distribution associated to a_k, as long as statistical independence between all variables is satisfied [23].

3. Results

We are ready to investigate the speckle development associated with the long-time dynamics of the Anderson model. Throughout the analysis we fix the input site to $n_0 = 1$ in Eqs. (2) and (3). A signature of a fully developed speckle is when the speckle contrast $C = \sigma_I/\langle I \rangle$ equals to unit (the exponential law applies for $I = |\psi|^2$), where σ_I is the standard deviation of the intensity. This is expected to be the case when the disorder W is weak, rendering amplitudes $|a_k|$ evenly distributed for all practical purposes.

Fig. 1 displays the contrast evaluated at many distances from the source n_0 for various disorder strengths W. We note that the increase of the disorder drives the statistics towards a sub-exponential regime ($C < 1$), especially at locations closer to the input site. This happens due to the spatial distribution of $a_k = v_{k,n_0} v_{k,n}$, with each $v_{k,n}$ decaying exponentially. As $n \approx n_0$, the phasor sum is dominated by fewer amplitudes.

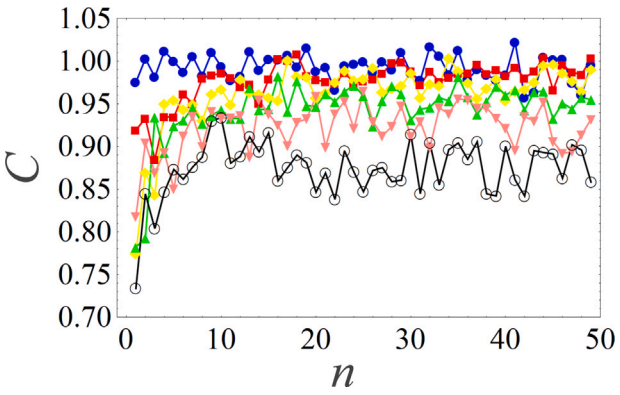

Fig. 1. Contrast $C = \sigma_I/\langle I \rangle$ of the intensity $I = |\psi|^2$ versus site n averaged over 10 independent realizations of disorder. In each case, the time evolution is realized up to $tJ = 10^5$, allowing for fast statistical convergence of the speckle contrast. System parameters are $N = 100$, with $W/J = 0.1$ (blue circles), 0.5 (red squares), 1 (yellow diamonds), 1.5 (green up triangles), 2 (pink down triangles), and 3 (open black circles). Numerical data were obtained via exact diagonalization of the Hamiltonian.

3.1. Rician-type distributions

To account for the sub-exponential statistics revealed by $C < 1$ in Fig. 1, we resort to compound Rician distributions as explained in the following.

In the case of a constant strong phasor with intensity I_0 interfering with a weaker random phasor sum – following an exponential distribution with mean s_r – the resulting intensity obeys the Rician distribution

$$f(I) = s_r^{-1} e^{-(I/s_r + r)} \mathcal{I}_0\left(2\sqrt{Ir/s_r}\right), \tag{5}$$

where $\mathcal{I}_0$ is the zeroth-order modified Bessel function of the first kind. This distribution is shaped by the ratio $r = I_0/s_r$ and becomes the exponential distribution in the limit $r \to 0$. The contrast of a Rician speckle is given by $C(r) = (1 + 2r)^{1/2}/(1 + r)$.

When localized modes are present, isolating a single dominant phasor will not ensure that the remaining terms (noise) amount to Rayleigh/exponential statistics. Instead, we may have to filter this noise from the dominant part of size μ. Hence, in general I_0 forms a speckle on its own and r becomes a random variable distributed according to $\rho(r)$. Finally, the output intensity can be described by compounding the Rician distribution with respect to r:

$$p(I) = \int_0^\infty dr\, f(I|r)\rho(r), \tag{6}$$

where $f(I|r)$ is the Rician distribution conditioned on knowledge about r.

In Fig. 2(a) we plot the intensity distribution for two distinct disorder strengths considering $n = 2$ (right next to the input site). As predicted, the sub-exponential statistics (red squares) is well described by a compound Rician distribution. Therein, we picked $\mu = 4$ largest amplitudes $|a_k|$ to build $\rho(r)$. To justify this choice, in 2(b) we evaluate the contrast C of the remaining phasor sum for various partitions of size $N - \mu$. As μ increases, C reaches a saturation level of $C \approx 0.85$ for $W = 4$ J. This is related to the finite localization length of the modes involved. Nevertheless, the noise can be effectively approximated as a fully developed speckle. Note that as the modes become more localized upon further increasing W, then $r \to \infty$ rendering the random phasor sum outside of the domain irrelevant. This is true for 1D and 2D systems featuring uncorrelated diagonal disorder, where every mode is exponentially localized. The situation is more involved when correlated disorder is considered [25]. In the case of weak disorder [blue circles in Fig. 2(a)], the distribution obeys the exponential law. Indeed, despite the form of $\rho(r)$, if r is vanishingly small the integral in Eq. (6) recovers the exponential distribution.

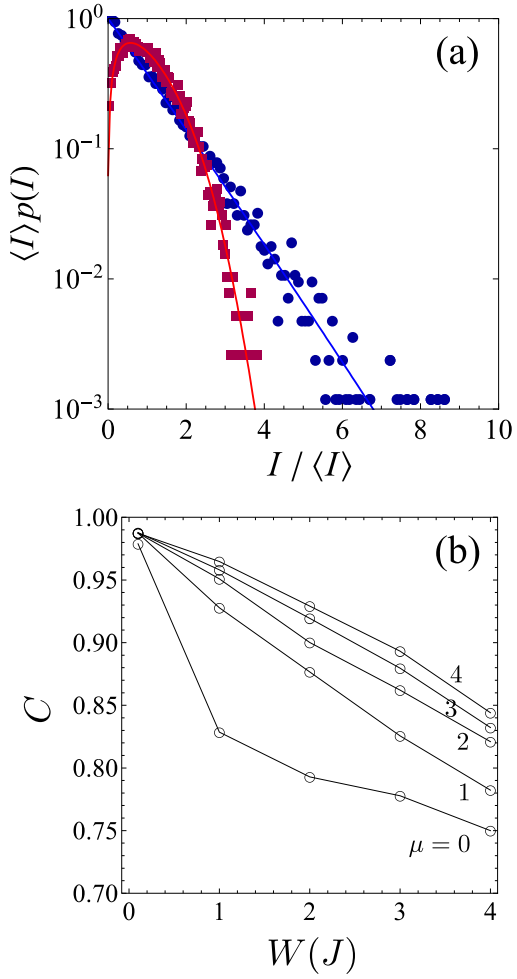

Fig. 2. (a) Probability density function of the intensity $I = |\psi|^2$ evaluated at $n = 2$ (with $n_0 = 1$) for $W = 0.1$ J (blue circles) and $W = 4$ J (red squares). The statistics is built from the exact numerical time evolution of a single realization of a periodic chain with $N = 100$ up to time $tJ = 10^6$. The fittings (solid lines) are obtained by compounding Rician distributions as in Eq. (6). The distribution for $r = I_0/s_r$, $\rho(r)$, was defined by setting aside $\mu = 4$ dominant amplitudes $|a_k|$ from the random phasor sum. Note that for weak disorder the exponential distribution (the limit $r \to 0$ of the Rician distribution) is recovered. (b) Contrast C of phasor sum formed by the remaining $N-\mu$ components versus disorder strength W for various μ (null μ means no filter). The contrast here is evaluated through random generation of the phases ϕ_k in an ensemble of 1000 resultant intensities and later averaged over 200 realizations of the disorder.

The takeaway message from the analysis above is that the likelihood of extreme events is less than predicted by exponential statistics when measurements are taken closer to a delta-like source, especially for stronger levels of the disorder.

3.2. Long-tailed distributions

So far we have been dealing with the intensity statistics $p(I)$ built over the time series of $I = I(n,t) = |\psi(n,t)|^2$ for single disorder realizations. Given a fixed set of coefficients a_k associated to random phases ϕ_k covering the whole circle (due to the truncated time evolution of the system) we could treat $I(n,t)$ as a local stochastic process.

We now move on to consider cases in which I is evaluated at a fixed (long) time and the statistics is performed over various disorder configurations and/or sites n. In these cases, we cannot be sure whether the mean intensity $s = s(n)$ will hold for independent disorder realizations with the same W. We henceforth discuss how this uncertainty gives rise to heavy-tailed statistics that describes speckles beyond the

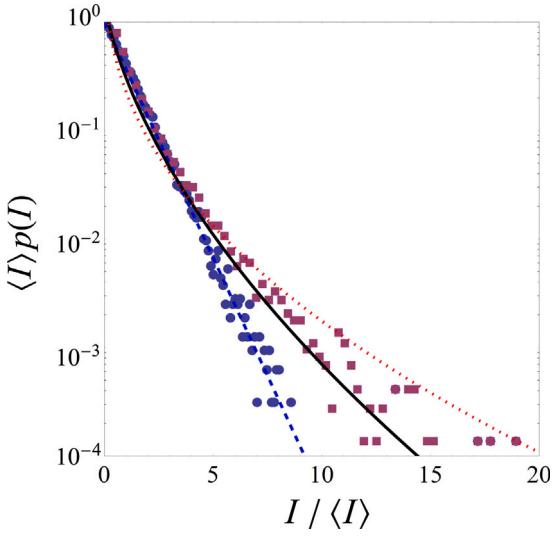

Fig. 3. Probability density function of the intensity $I = |\psi|^2$ evaluated at $n = 50$ and $tJ = 5000$ (now fixed). Data is obtained from 10^4 independent realizations of disorder considering $N = 100$ sites. Disorder strengths are $W = 0.1$ J (blue circles) and $W = 2$ J (red squares). The exponential fitting is represented by the blue dashed line. The heavy tailed curves are K-distributions given by Eq. (9) with $M = 3$ (black solid line) and $M = 1$ (red dotted line) . The K-distribution approaches the exponential distribution as $M \to \infty$.

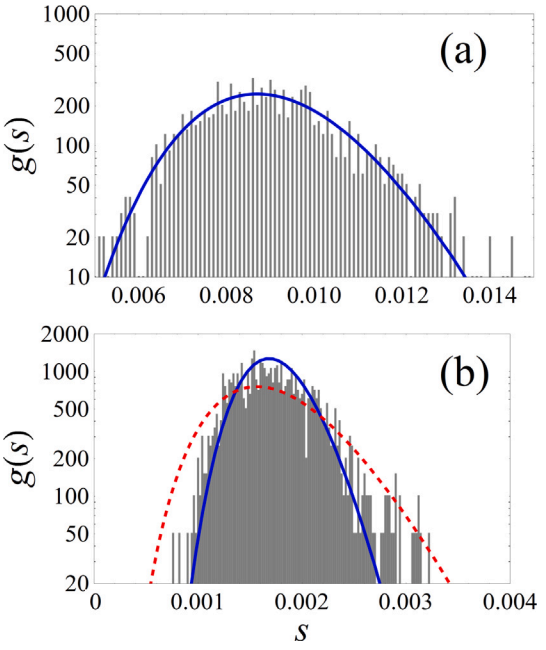

Fig. 4. Distribution $g(s)$ of the mean intensities $s = \langle I\rangle$ at $n = 50$ and $tJ = 5000$ averaged over 30 independent outputs of an ensemble of 3000 independent realizations of disorder and $N = 100$. Disorder strengths are (a) $W = 0.1$ J and (b) $W = 2$ J. Blue-solid and red-dashed lines are fittings obtained from the Erlang function [Eq. (8)] with $M = 30$ and $M = 10$, respectively.

exponential regime. For convenience, we assume that a given intensity measurement is a random variable originated from an exponentially-distributed process $I(n,t)$. Again, this is valid when the disorder is weak and/or n is not very close to n_0.

Next, we follow the approach outlined in [15], which describes linear rogue waves observed in microwave transport through disordered scatterers. We begin by defining the intensity distribution as the average of the conditional density function $p(I|s) = s^{-1}e^{-I/s}$ over the

distribution of the mean intensity $g(s)$:

$$p(I) = \int_0^\infty ds\ p(I|s)g(s), \tag{7}$$

where a specific form for $g(s)$ should therefore be in order.

The resulting distribution of a sum of random variables is the convolutions of the individual parts. In the case of a sum of M independent exponentially-distributed random variables X_i, each with associated mean s_i, a hypoexponential distribution with M parameters s_i^{-1} is obtained. But here we take a simpler route and consider equal $s_i = s_0$. (The validity of such an approximation will be discussed shortly.) In this case the resulting distribution is an Erlang density function with shape and scale parameters M and M/s_0, respectively:

$$g(s) = \frac{M^M (\frac{s}{s_0})^{M-1} e^{-Ms/s_0}}{s_0 \Gamma(M)}, \tag{8}$$

where $\Gamma(M) = (M-1)!$. This function is a special case of the gamma density function where M is a positive integer. Also note that it converges to a delta function as M increases (as expected given a well defined mean intensity s_0 is implied).

Plugging Eq. (8) back into Eq. (7), the integral can be solved as

$$p(I) = \frac{2M^{\frac{M+1}{2}}}{s_0 \Gamma(M)} \left(\frac{I}{s_0}\right)^{\frac{M-1}{2}} K_{M-1}\left(2\sqrt{\frac{MI}{s_0}}\right), \tag{9}$$

where K_M is the modified Bessel function of the second kind of order M. The above equation is known as the K-distribution and is commonly used to describe radiation scattering. Note that a very large M reduces it to $p(I) = s_0^{-1} e^{-I/s_0}$ as $g(s) \to \delta(s - s_0)$. In other words, a large number of measurements should increasingly provide knowledge over s_0. Physically, it makes sense if there is indeed a well defined s_0 so as to justify the approximation that led us to Eq. (8). This happens to be the case when weak disorder is considered, as shown in Fig. 3 (dashed blue curve) for $n = 50$ (far away from $n_0 = 1$), where the exponential distribution remains valid. Considering the same parameters, in Fig. 4(a) we confirm that the Erlang distribution $g(s)$ fits well to the numerical data made up of thousands of independent averages realized over sets of $M = 30$ distinct samples. Such a value for the shape parameter renders a distribution barely distinguishable from an exponential one.

On the other hand, strong disorder inevitably yields to heavy-tailed statistics as seen in Fig. 3 (red squares). Now, Eq. (9) fits well with the numerical data (red squares) as long as M is set to lower values in order to compensate for the non-homogeneity of s_i. At first, we may assume complete ignorance and choose $M = 1$, which gives $g(s) \sim e^{-s}$, to get the longest tail (see red dotted curve in Fig. 3). As this might overestimate the onset of extreme outcomes, a more careful analysis can be made by looking directly at $g(s)$. In Fig. 4(b) we note that, for example, $M = 30$ fails to account for the extreme averages [not as rare as in Fig. 4(a)]. We can reach out for those values by decreasing M, with the small price of deviating from the regular events.

To gain a better perspective on how the speckle fluctuations build up with the disorder, in Fig. 5 we display C versus W at various locations n. Note that when $n = 2$ (closer to the input), the statistics remains close to an exponential ($C \approx 1$) for the whole range of W. Hence, we see that the Rician-type distribution followed by I is robust against disorder fluctuations. As both W and n increase, speckle fluctuations become more pronounced, resulting in $C > 1$. The K-distribution can then be chosen provided $C(M) = \sqrt{(M+2)/M}$, especially in the low disorder range such that $I(t)$ can be approximated as an exponentially-distributed random process.

We now obtain the statistics for the whole chain at once. Now, in addition to not knowing the rate of the exponential processes (or Rice-type processes for n close enough to the input) occurring locally, we are also not certain about the distance between the input and output locations, n and n_0, respectively. In Fig. 6 we compare results obtained for weak ($W = 0.1$ J) and intermediate ($W = 1$ J) disorder strengths and confirm a departure from the exponential regime in the latter case.

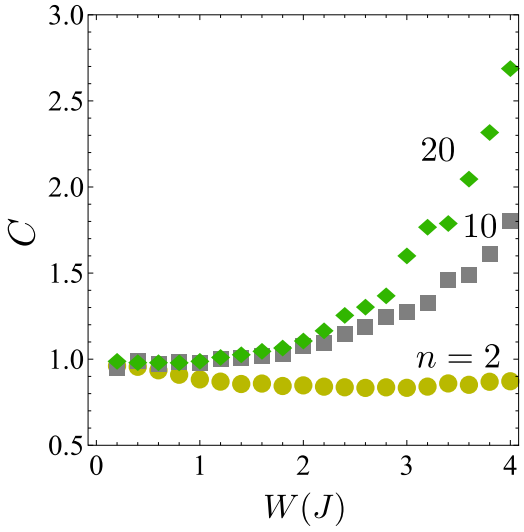

Fig. 5. Contrast C versus disorder strength W at fixed time $tJ = 10^6$ and locations n as indicated. The number of independent disorder realizations was 10^4 for $N = 50$.

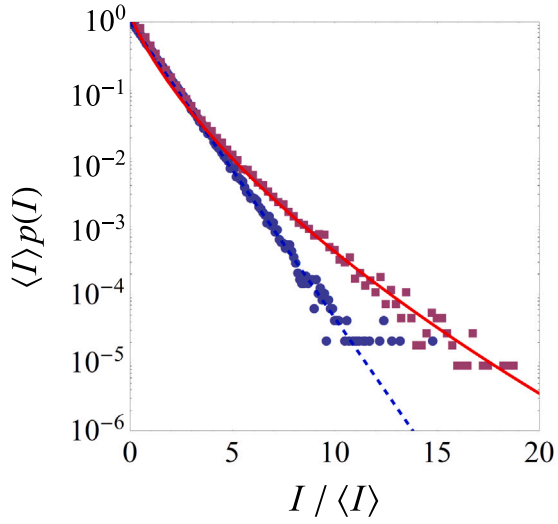

Fig. 6. Probability density function of the intensity $I = |\psi|^2$ evaluated for all n over a chain with $N = 50$ sites at time $tJ = 5000$ for 10^5 independent realizations of the disorder, with $W = 0.1$ J (blue circles) and $W = 1$ J (red squares). The blue-dashed- and red solid lines represent the exponential distribution $\sim e^{-I}$ and the K-distribution with $M = 5$, respectively.

The same reasoning used to justify the K-distribution in Eq. (9) can be employed to include both disorder realizations and positions n if we ignore that sites closer the input obey Rician-type statistics. Once again, the resulting heavy-tailed profile is well described by the K-distribution as long as we cope with our lack of knowledge by keeping M low enough.

To summarize the findings above, we conclude that heavy-tailed statistics emerge whenever $g(s)$ cannot approach a delta function in the limit of large M.

3.3. Rogue wave events

In this last section, we discuss how the speckle statistics discussed so far is related to the occurrence of rogue waves. First, we mention that any criterion for deciding what is a rogue wave and what is not will always be arbitrary to some extent. Some authors define the rogue wave threshold I_{RW} as two times the mean the largest 1/3 of events

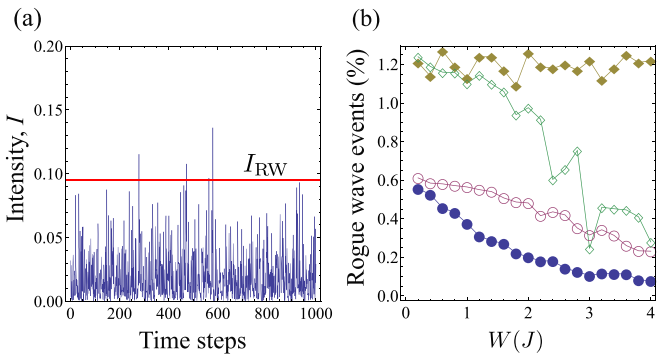

Fig. 7. (a) Single (typical) realization of the intensity time evolution for $N = 50$, $n = 2$, $W = 0.1$ J, up to $tJ = 10^6$ divided into 10^3 steps. The horizontal line stands for the rogue-wave threshold $I_{RW} = \langle I \rangle + 4\sigma_I$, defined for the corresponding wave record. (b) Number of rogue wave events versus disorder strength W considering $n = 2$ (filled symbols), $n = 20$ (empty symbols). The circles represent the average number of rogue events recorded over time for an individual disorder realizations [such as the one depicted in (a)]. The diamonds cover the statistics resulting from an ensemble of 5×10^4 disorder realizations with the intensities evaluated at a fixed time $tJ = 10^6$. The thresholds I_{RW} were set accordingly.

within a dataset (known as the significant wave height) [21,22,25,29]. Others define it as any wave event that exceeds the average by a given amount of standard deviations [4,30]. Here, we will use the latter by setting $I_{RW} = \langle I \rangle + 4\sigma_I = (1 + 4C)\langle I \rangle$, in terms of the speckle contrast.

Fig. 7(a) shows a typical realization of a temporal evolution resembling a speckle pattern. The few intensities (out of 1000) that crosses the horizontal line given by I_{RW} are classified as rogue wave events. In Fig. 7(b) we display the percentage of those in various cases. When the wave record is based on individual realizations of the disorder (circles), the rate of rogue wave events diminishes upon increasing W, especially when the probe is right next to the input location (filled circles). As addressed earlier, this is a consequence of the localization of the modes involved, what effectively reduces the speckle fluctuations, favoring Rician statistics. When the intensities are recorded from an ensemble of disorder realizations at a fixed point in space and time, the rate of rogue events measured next to the input displays no definite trend with increasing W. Contrarily, if the probe location is far, the occurrence of rogue waves becomes less likely. Interestingly, this happens despite the increase of the speckle contrast C with W as shown in Fig. 5 for $n > 2$. Nevertheless, we must recall that $I_{RW} = I_{RW}(C)$ and thus long-tailed distributions ($C > 1$) will typically feature higher rogue-wave thresholds as well, making them more difficult to occur. By the same argument, we can understand why the likelihood of rogue wave events based on an ensemble of disorder realizations does not change with W for $n = 2$ in Fig. 7 (filled diamonds). There is a balance between disorder-induced fluctuations in the random variable I and its own sub-exponential speckle statistics (cf. Fig. 5).

4. Conclusions

A parallel between random phasor sums employed to describe optical speckles and the Hamiltonian dynamics of an Anderson chain has been put forward. We found that the intensity statistics evaluated closest to the input site n_0 deviates from the exponential law towards a Rician-type distribution as disorder grows, thereby diminishing the number of rogue wave events. But we have also seen that the speckle statistics ultimately depends on how the data is arranged. When distinct disorder realizations are considered at once, K-distributed speckles result from compounding exponential distributions with different rates. In this case, the opposite happens: rogue waves are more likely to occur at sites closer to n_0. The reason for this is that higher speckle contrasts results in higher rogue-wave thresholds I_{RW} making occurrences rarer at $n \gg n_0$.

Our findings can be readily realized using, e.g., coupled photonic waveguides [21,31–33] or chains of LC contours with fluctuating resonant frequencies [34], where direct mappings onto tight-binding Hamiltonians are in order.

For instance, in Ref. [21], Rivas et al. observed rogue waves arising from single-site excitations in photonic lattices (of size $N = 81$) written with femtosecond lasers. By means of the natural evolution of the system, they were able to record rogue waves by counting the intensities across the sites (which naturally results in a long-tailed distribution) for a given disorder realization. The authors also highlighted that rogue-wave statistics is highly influenced by the kind of wave record or filtering. Despite their experiment being limited to short distances (time steps in our case) and disorder samples, some remarkable conclusions could be drawn, including that weak disorder is ideal for observing rogue waves. Here, in Fig. 7(a) we have discussed this behavior in detail from the perspective of two kinds of wave records: over a single disorder realization and over an ensemble of such realizations. With that, we could also draw attention to the counter-intuitive behavior of the rogue wave statistics against W. Finally, we mention that our findings could be realized in much shorter time spans. Our typical maximum time was chosen out of numerical convenience, allowing for fast statistical convergence of the speckle contrast C. In a practical realization, limitations due to the maximum time or propagation distance can be addressed by considering alternative input configurations.

Possible extensions of this work include investigating the influence correlated disorder [25] and initial conditions featuring modulated phases [35], factors known to have dramatic influence in the occurrence of rogue events. Note that initial states in superposition renders a sum over random phasor sums which generally does not yield to a fully developed speckle regime [25]. The possibilities are thus set to uncover novel features in the dynamics of disordered quantum systems through the lens of heavy-tailed phenomena.

Funding

This research received funding from CNPq, CAPES, and FAPEAL (Alagoas State agency).

CRediT authorship contribution statement

M.F.V. Oliveira: Visualization, Methodology, Investigation. **A.M.C. Souza:** Writing – original draft, Investigation, Conceptualization. **M.L. Lyra:** Writing – review & editing, Supervision, Funding acquisition, Formal analysis. **F.A.B.F. de Moura:** Writing – original draft, Methodology, Investigation, Funding acquisition, Conceptualization. **G.M.A. Almeida:** Writing – review & editing, Writing – original draft, Validation, Supervision, Methodology, Investigation, Data curation, Conceptualization.

Declaration of competing interest

The authors declare that they have no known competing financial interests or personal relationships that could have appeared to influence the work reported in this paper.

Data availability

Data will be made available on request.

Acknowledgment

We acknowledge P. A. Brandão for relevant insights. All authors have read and agreed to the published version of the manuscript.

References

[1] K. Dysthe, H.E. Krogstad, P. Müller, Oceanic rogue waves, Annu. Rev. Fluid Mech. 40 (2008) 287.

[2] D.R. Solli, C. Ropers, P. Koonath, B. Jalali, Optical rogue waves, Nature 450 (2007) 1054.

[3] J.M. Dudley, G. Genty, A. Mussot, A. Chabchoub, F. Dias, Rogue waves and analogies in optics and oceanography, Nat. Rev. Phys. 1 (2019) 675.

[4] C. Bonatto, M. Feyereisen, S. Barland, M. Giudici, C. Masoller, J.R.R. Leite, J.R. Tredicce, Deterministic optical rogue waves, Phys. Rev. Lett. 107 (2011) 053901.

[5] F. Baronio, M. Conforti, A. Degasperis, S. Lombardo, M. Onorato, S. Wabnitz, Vector rogue waves and baseband modulation instability in the defocusing regime, Phys. Rev. Lett. 113 (2014) 034101.

[6] L. Liu, B. Tian, X.-Y. Wu, Y. Sun, Higher-order rogue wave-like solutions for a nonautonomous nonlinear Schrödinger equation with external potentials, Physica A 492 (2018) 524.

[7] G. Xu, A. Chabchoub, D.E. Pelinovsky, B. Kibler, Observation of modulation instability and rogue breathers on stationary periodic waves, Phys. Rev. Res. 2 (2020) 033528.

[8] C. Bayındır, Rogue quantum harmonic oscillations, Physica A 547 (2020) 124462.

[9] N. Akhmediev, J.M. Soto-Crespo, A. Ankiewicz, How to excite a rogue wave, Phys. Rev. A 80 (2009) 043818.

[10] M. Onorato, A.R. Osborne, M. Serio, S. Bertone, Freak waves in random oceanic sea states, Phys. Rev. Lett. 86 (2001) 5831.

[11] L.H. Ying, Z. Zhuang, E.J. Heller, L. Kaplan, Linear and nonlinear rogue wave statistics in the presence of random currents, Nonlinearity 24 (2011) R67.

[12] A. Safari, R. Fickler, M.J. Padgett, R.W. Boyd, Generation of caustics and rogue waves from nonlinear instability, Phys. Rev. Lett. 119 (2017) 203901.

[13] F.T. Arecchi, U. Bortolozzo, A. Montina, S. Residori, Granularity and inhomogeneity are the joint generators of optical rogue waves, Phys. Rev. Lett. 106 (2011) 153901.

[14] N. Lv, J. Li, X. Yuan, R. Wang, Controllable rogue waves in a compressible hyperelastic plate, Phys. Lett. A 461 (2023) 128639.

[15] R. Höhmann, U. Kuhl, H.-J. Stöckmann, L. Kaplan, E.J. Heller, Freak waves in the linear regime: A microwave study, Phys. Rev. Lett. 104 (2010) 093901.

[16] J.J. Metzger, R. Fleischmann, T. Geisel, Universal statistics of branched flows, Phys. Rev. Lett. 105 (2010) 020601.

[17] S. Barkhofen, J.J. Metzger, R. Fleischmann, U. Kuhl, H.-J. Stöckmann, Experimental observation of a fundamental length scale of waves in random media, Phys. Rev. Lett. 111 (2013) 183902.

[18] J.J. Metzger, R. Fleischmann, T. Geisel, Intensity fluctuations of waves in random media: What is the semiclassical limit? Phys. Rev. Lett. 111 (2013) 013901.

[19] J.J. Metzger, R. Fleischmann, T. Geisel, Statistics of extreme waves in random media, Phys. Rev. Lett. 112 (2014) 203903.

[20] C. Liu, R.E.C. van der Wel, N. Rotenberg, L. Kuipers, T.F. Krauss, A. Di Falco, A. Fratalocchi, Triggering extreme events at the nanoscale in photonic seas, Nat. Phys. 11 (2015) 358.

[21] D. Rivas, A. Szameit, R.A. Vicencio, Rogue waves in disordered 1d photonic lattices, Sci. Rep. 10 (2020) 13064.

[22] A.R.C. Buarque, W.S. Dias, F.A.B.F. de Moura, M.L. Lyra, G.M.A. Almeida, Rogue waves in discrete-time quantum walks, Phys. Rev. A 106 (2022) 012414.

[23] J. Goodman, Speckle Phenomena in Optics: Theory and Applications, in: Press Monographs, SPIE Press, 2020.

[24] E. Abrahams, P.W. Anderson, D.C. Licciardello, T.V. Ramakrishnan, Scaling theory of localization: Absence of quantum diffusion in two dimensions, Phys. Rev. Lett. 42 (1979) 673.

[25] A.R.C. Buarque, W.S. Dias, G.M.A. Almeida, M.L. Lyra, F.A.B.F. de Moura, Rogue waves in quantum lattices with correlated disorder, Phys. Rev. A 107 (2023) 012425.

[26] M.F.V. Oliveira, F.A.B.F. de Moura, A.M.C. Souza, M.L. Lyra, G.M.A. Almeida, Non-rayleigh signal of interacting quantum particles, Phys. Rev. A 108 (2023) 023520.

[27] E. Kogan, M. Kaveh, Random-matrix-theory approach to the intensity distributions of waves propagating in a random medium, Phys. Rev. B 52 (1995) R3813.

[28] A.D. Mirlin, R. Pnini, B. Shapiro, Intensity distribution for waves in disordered media: Deviations from rayleigh statistics, Phys. Rev. E 57 (1998) R6285.

[29] C. Kharif, E. Pelinovsky, A. Slunyaev, Rogue Waves in the Oceans, Springer-Verlag Berlin Heidelberg, 2009.

[30] C. Bonatto, S.D. Prado, F.L. Metz, J.R. Schoffen, R.R.B. Correia, J.M. Hickmann, Super rogue wave generation in the linear regime, Phys. Rev. E 102 (2020) 052219.

[31] T. Schwartz, G. Bartal, S. Fishman, M. Segev, Transport and anderson localization in disordered two-dimensional photonic lattices, Nature 446 (2007) 52.

[32] Y. Chen, X. Chen, X. Ren, M. Gong, G.-c. Guo, Tight-binding model in optical waveguides: Design principle and transferability for simulation of complex photonics networks, Phys. Rev. A 104 (2021) 023501.

[33] J. Yang, Y. Li, Y. Yang, X. Xie, Z. Zhang, J. Yuan, H. Cai, D.-W. Wang, F. Gao, Realization of all-band-flat photonic lattices, Nature Commun. 15 (2024) 1484.

[34] E. Diez, F. Izrailev, A. Krokhin, A. Rodriguez, Symmetry-induced tunneling in one-dimensional disordered potentials, Phys. Rev. B 78 (2008) 035118.

[35] H. Frostig, I. Vidal, R. Fischer, H.H. Sheinfux, Y. Silberberg, Observation of rogue events in non-markovian light, Optica 7 (2020) 864.